Calculation of Linear Added mass Coefficients for a submerged vehicle Using Numerical and Analytical Methods

A. Shadlaghani[1], Sh. Mansoorzadeh[2]

[1]Graduated M.Sc. student, Isfahan University of Technology; a.shadlaghani@me.iut.ac.ir
[2]Assistant Prof, Isfahan University of Technology /Subsea R&D center; shahriar@cc.iut.ac.ir

Abstract
Added mass is the virtual additional mass of an object when it is accelerated relative to the surrounding fluid. The present paper documents both numerical and analytical methods for computing the added mass coefficients of submerged vehicles. A new numerical method is described to calculate the linear coefficients in axial and lateral directions. The method is firstly validated by comparing its results with the known results for a sphere. Numerical results show that the added mass coefficients are independent from accelerations values. In addition, an analytical method which is called equivalent ellipsoid is explained to approximate the added mass coefficients. In this approach, various components of vehicle are separately replaced by ellipsoids whose dimensions are optimally determined by measuring the moments of inertia. Comparison of the obtained results with available and published experimental reports of DARPA SUBOFF submarine shows the simplicity and accuracy of the numerical and even analytical approaches.

Keywords: Added Mass, Submarine, Linear Accelerated Motions, Equivalent Ellipsoids

Introduction

In recent years, underwater vehicles have been used in various fields such as military, oceanographic, exploration, etc. In order to investigate the dynamic behavior of these vehicles, their motion equations should be solved. The external force in these equations consists of the hydrostatic, hydrodynamic, thrust, and control surfaces forces. Unsteady motion of submerged vehicles in water changes the kinetic energy of the surrounding fluid. The acting force due to this phenomenon is called added mass force. Added mass force is the fluid weight added to the object; thus, the second law of Newton can be written as $F = (m + m_a)a$.

Traditionally, potential flow theory, Semi-empirical and experimental methods have been used to predict added mass coefficients. Perrault [1] estimated the total components of added mass matrix for an AUV by an analytical approach. Lin and Liao [2] calculated the added mass coefficients of a complicated underwater vehicle using fast multiple boundary element method (FMBEM), and concluded that their method was computationally more efficient than the traditional BEM. Extending potential flow and strip theories as far as possible, Watt [3] introduced an analytical method in which various components of submersibles were replaced by ellipsoids. Watt showed that the overall forces in an ideal fluid were linear in term of the kinetic energy of flow field; therefore, the total added mass force of a submersible could be obtained from linear summation of each component force.

Nowadays, CFD methods are more utilized to the hydrodynamic applications due to development of computer sciences. Using Reynolds Averaged Navier-Stoks (RANS) techniques, simulation of the planar mechanism motion (PMM) has been widely applied to compute the added mass coefficients of underwater vehicles. For instance, Zhang [4] simulated the PMM test numerically and obtained the corresponding hydrodynamic coefficients to evaluate the maneuverability of a submersible during design stages. Phillips [5] used numerical simulations to replicate the horizontal PMM tests for an AUV designed at the National Oceanography Center of Southampton. In another work, focusing on the hydrodynamic performance, Jinxin [6] simulated PMM tests and oblique sailing by a commercial software. He also investigated the effect of appendages on the motion performance of AUV. Hochbaum [7] simulated PMM tests numerically for the NSTL ferry and compared his results by experimental tests. Lee [8] calculated the added mass coefficients for an unmanned underwater vehicle by simulation of the vertical plannar mechanis motion, and compared his results with experimental method.

It's obvious that the PMM simulations are the customary procedure in calculating added mass coefficients, but frequency and amplitude of oscillations can influence the the output results. In order to avoid these effects, in this paper, an alternative numerical method is explained to calculate the linear added mass coefficients. An analytical approach is also introduced to determine the same coefficients. Disregarding the viscous effects and time dependent of flow nature causes these methods have been used to estimate the hydrodynamic derivatives.

Motion equations and description of model

Motion of an underwater vehicle is discribed by definition of two coordinate systems. Displacements are defined in the inertial frame coincided to the earth frame, while the motion equations are described in the body-fix frame.

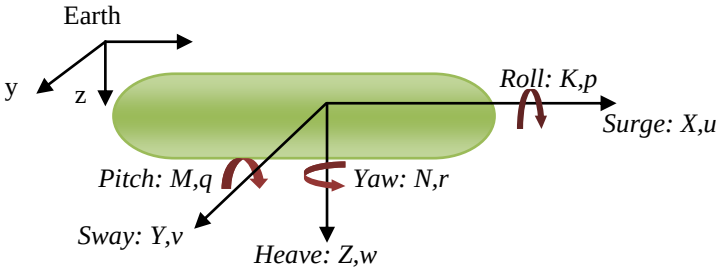

Figure 1: Coordinate systems and definitions

[u v w p q r] are the linear and angular velocities and [X Y Z K M N] are the acted forces and moments. The motion equations for linear motion in the horizontal and vertical plane are simplified to the linear equations defined as:

$$\begin{aligned} &Surge: (m - X_{\dot{u}})\dot{u} = X_u(u+U) + X_{prop} \\ &Sway: (m - Y_{\dot{v}})\dot{v} + (mx_G - Y_{\dot{r}})\dot{r} = Y_v v + (Y_r - mU)r + Y_\delta \delta \\ &Heave: (m - Z_{\dot{w}})\dot{w} - (mx_G + Z_{\dot{q}})\dot{q} = Z_w w + (Z_q + mU)q + Z_\delta \delta \end{aligned} \quad (1)$$

m and C_G = [x_G,y_G,z_G] are the mass and gravity center of vehicle. δ and U are the control surface angle and towing velocity of the vehicle respectively. Note that, $X_{\dot{u}} = \frac{\partial X}{\partial \dot{u}}$, $X_u = \frac{\partial X}{\partial u}$ are the hydrodynamic derivatives including added mass and damping coefficients. For example, $X_{\dot{u}}$ is the added mass in x direction because of the surge motion. In this paper, DARPA SUBOFF is chosen for investigations because its experimental data is available. Geometrical parameters of submarine are given in table1.

Table 1: Geometric parameter of SUBOFF

Total length	4.356 (m)
maximum diameter	0.508 (m)
Volume of displacement	0.718 (m^3)
Wetted surface	6.33 (m^2)

This submarine was designed in the David Taylor research center (DTRC), and various experiments were carried out to determine its hydrodynamic coefficients [9].

Figure 2: sketch of DARPPA SUBOFF submarine

Numerical procedure

In order to calculate the added mass of a submerged model, two kinds of motions including constant velocity and constant acceleration should be imposed successively. If F_1 is the needed force for towing the model with constant velocity, this force is evidently equivalent to the drag force. Afterwards, if this model is towed with a constant acceleration, the towing force (F_2) should overcome the drag force as well as an extra force due to accelerating the model and surrounding fluid. Note that, velocities are equivalent together for both stages at the conversion time of motion. The difference between F_1 and F_2 at the conversion time gives the amount of added mass.

$$F_2 - F_1 = (m + m_a)a \quad \Rightarrow \quad m_a = \frac{F_2 - F_1}{a} - m \quad (2)$$

In Eq.2, m and a are the model fluid mass and acceleration values respectively. m_a is the added mass of carried fluid in the direction of motion.

Analytical approach

In this section, an analytical method based on the potential flow theory is to be clarified to compute the diagonal added mass coefficients of underwater vehicles. Short descriptions of the main stages to determine the added masses are

- Aproximating the components of the underwater vehicle as a series of ellipsoids
- Representing the optimum dimensions of each ellipsoid
- Calculating the added mass of the replacement ellipsoids separately
- Linear summation of the calculated added masses

Moment of inertia as a mathematical property of geometry can be a good criterion for obtaining the best dimensions of the replaced ellipsoids in order to maximize the accuracy of calculations. Because the hull is axisymmetric, it's sufficient to determine two axial and lateral diameters of the replaced ellipsoid using the area moment of inertia. Similarly, in appendages case, because an appendage primarily affects forces perpendicular to its planform area, an ellipse firstly replaces the planform. The maximum thickness of appendage is considered as the third diameter of replaced ellipsoid.
Now, Consider an ellipsoid totally submerged with the origin at the center of the ellipsoid as:

$$\frac{x^2}{a^2}+\frac{y^2}{b^2}+\frac{z^2}{c^2}=1 \tag{3}$$

After computing the dimensions, the next step is to determine the added mass coefficients for the ellipsoids. Following formula are represented for calculating the linear added mass derivatives.

$$X_{\dot{u}}=k_{11}m \qquad Y_{\dot{v}}=k_{22}m \qquad Z_{\dot{w}}=k_{33}m \tag{4}$$

Korotkin [10] introduced Lamb's k-factors as:

$$k_{11}=\frac{A_0}{2-A_0} \qquad k_{22}=\frac{B_0}{2-B_0} \qquad k_{33}=\frac{C_0}{2-C_0} \tag{5}$$

Where, A_0, B_0, C_0 are the constants that describe the relative proportions of the ellipsoid.

$$\begin{aligned} A_0&=abc\int_0^\infty \frac{du}{(a^2+u)\sqrt{(a^2+u)(b^2+u)(c^2+u)}}\\ B_0&=abc\int_0^\infty \frac{du}{(b^2+u)\sqrt{(a^2+u)(b^2+u)(c^2+u)}}\\ C_0&=abc\int_0^\infty \frac{du}{(c^2+u)\sqrt{(a^2+u)(b^2+u)(c^2+u)}} \end{aligned} \tag{6}$$

Watt [3] showed that the interference effects between various components had a negligible influence in computing the diagonal coefficients. Thus, the total added mass can be written as the linear summation of each component contribution.

$$\begin{aligned} X_{\dot{u}}&=(K_{11}m)_{hull}+(K_{11}m)_{sail}+(K_{11}m)_{control-surfaces}\\ Y_{\dot{v}}&=(K_{22}m)_{hull}+(K_{22}m)_{sail}+(K_{22}m)_{control-surfaces}\\ Z_{\dot{w}}&=(K_{33}m)_{hull}+(K_{33}m)_{sail}+(K_{33}m)_{control-surfaces} \end{aligned} \tag{7}$$

Numerical analysis

The motion of fluid is modeled by RANS equations to determine the flow field variables (u,v,w,p). For an incompressible and isothermal flow, these equations are

$$\begin{aligned} &\frac{\partial \overline{u}_i}{\partial x_i}=0\\ &\frac{\partial \overline{u}_i}{\partial t}+\frac{\partial(\overline{u_i u_j})}{\partial x_j}=f_i-\frac{1}{\rho}\frac{\partial P}{\partial x_i}+\frac{\partial}{\partial x_j}\left(\upsilon\left(\frac{\partial \overline{u}_i}{\partial x_j}+\frac{\partial \overline{u}_j}{\partial x_i}\right)\right)-\frac{\partial \overline{u_i' u_j'}}{\partial x_j} \end{aligned} \tag{8}$$

The Reynolds stresses ($u_i' u_j'$) are additional unknowns appeared by the averaging procedure. Turbulence models relate the Reynolds stresses to the averaged flow quantities in order to close the system of governing equations. The K−ε model is a common turbulence model for engineering simulations, but it is weak to introduce the location of the separation point. An alternative model is Shear Stress Transport (SST). This model synthesizes both k-ω and k-ε model to solve the Reynolds stresses near the wall and out of the boundary layer respectively. The finite volume method is implemented to solve the unsteady NS equations in all simulations. The advection term and turbulence equations are solved numerically using the high-resolution scheme. The convergence limitation is also set at 10^{-5} for all simulations.

Mesh definition

Unstructured grids are used to generate elements in the entire fluid domain. This kind of grids has a better adaptability in complicated geometry. Prism elements are used inside the boundary layer for increasing the number of elements and solution accuracy. Thus, it is necessary to estimate the thickness of boundary layer and arrangement of grids layers near the wall. Thickness of boundary layer and the first layer for a blunt body with desired y^+ can be estimated

$$\delta = 0.035L(\mathrm{Re})^{-1/7} \tag{9}$$

$$\Delta y = L\, y^{+} \sqrt{80}\ \ \mathrm{Re}_{L}^{-13/14} \tag{10}$$

L is the flow length scale and the Reynolds number is calculated based on this scale. One of the main steps in the CFD analysis is checking the sensitivity of solution to the number of elements. Because the viscous parameter affects on the size of grids, it is better to investigate the variation of the skin drag coefficient. The grid study is performed in the way that the number of elements should be increased until the variations of C_f become negligible. Table2 shows the results of a typical grid study in the surge motion of submarine.

Table 2: Typical grid study for the Suboff in surge motion

	Coarse	Medium	Fine	Fine (1)	Fine (2)
Total element	833864	1106616	1259877	1878225	2534171
C_f	0.0035	0.0033	0.0031	0.0031	0.0031

The results of fine, fine (1), and fine (2) grids are identical; therefore, it is computationally appropriate to use fine grid for this case.

Numerical simulation

First, simulation is accomplished for a sphere with radius of 1m to ensure the accuracy of proposed numerical procedure. On the other hand, it's essential to find the correct values of the force at the conversion time of motion, and simulation of sphere can help us in making this decision. Figure3 shows the dimensions, grids, and boundary conditions for sphere simulation.

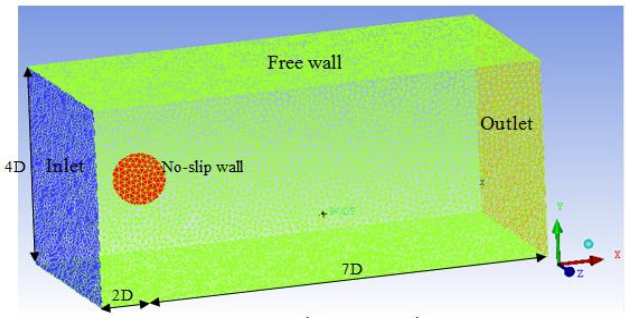

Figure 3: Dimensions and boundary condition for sphere simulation

The boundary conditions consist of time dependent velocity for the inlet, zero static pressure for the outlet, no-slip wall for sphere surface, and free slip wall for outer domain wall. Table3 shows the results of grid study for a series of refinement grids.

Table 3: Typical grid study for the sphere motion

Case study	Coarse	Medium	Fine	Fine(1)	Fine(2)
Total element	1318553	1618887	2009970	2234049	2729871
C_f	0.0459	0.0448	0.0441	0.044	0.044

Here again, the fine grid is computationally more efficient relative to the other grids. Now, the sphere is moved with speed of $V_{(t)}$ for five seconds, and the normal acted force is simultaneously monitored as Fig4.

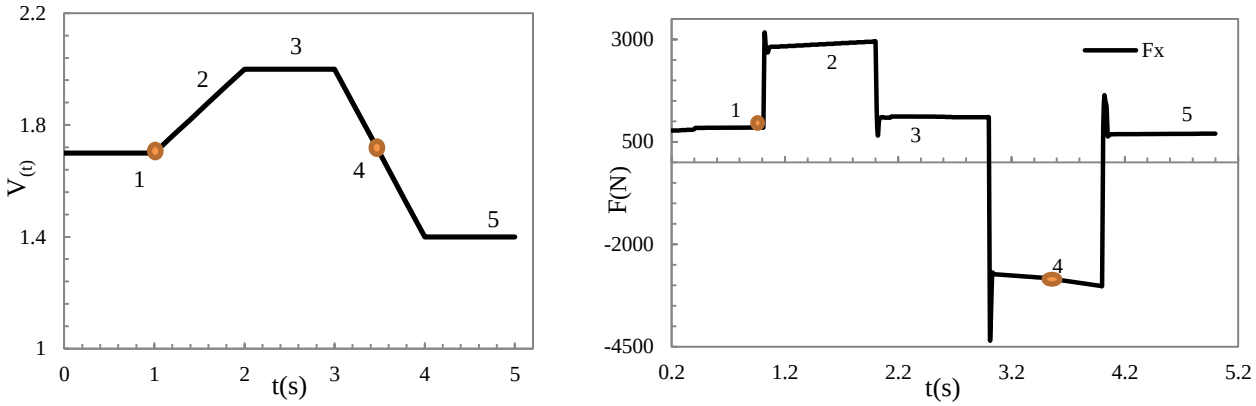

Figure 4: The acted force on the sphere due to velocity

As soon as the motion type is changed, the fluid flow through the model cannot accord with the new motion immediately. This physical phenomenon called history effect has been observed in the experimental tests [11]. Force oscillations that created by history effects of fluid make it difficult to get the correct force at the conversion time of motions. For solving this problem, in addition to the first stage, at the t=3.5s (stage 4) velocity is 1.5m/s except that in this stage, motion is accelerated without history effect. As a result, the added mass obtained from the first and fourth stages must be equivalent to obtained value from the first and second stages. Comparison shows that the force after oscillation should be considered as the force of second stage; therefore, the forces after oscillations are the correct values for each stage. Table4 shows the computed forces and related added masses for each stage separately.

Table 4: Calculated forces and added masses for sphere

	F_D(N)	F_2(N)	$m_a(kg)=\frac{F_2-F_D}{a}-m$	$C=\frac{m_a}{\rho V}$
Stage1-2	850	2750	2157.1	0.51
Stage2-3	1100	2950	1990.4	0.48
Stage3-4	1100	2690	2140.4	0.51
Stage4-5	700	-2992	1977.1	0.47
Stage1-4	850	-2820	1940.5	0.46

The added mass coefficients values obtained from the table 4 are close to the expected result for sphere (C=0.5); therefore, present numerical procedure has a good accuracy. Hereby, according to Eq.11, the SUBOFF submarine first moves with constant acceleration, and at the end of this stage, it moves with constant velocity.

$$V=\begin{cases}0.5t & t\le 1\\ 0.5 & t>1\end{cases} \tag{11}$$

Other boundary conditions are similar to the sphere case. Note that, this simulation is separately replicated in the *x,y,z* directions for calculating the $X_{\dot{u}}, Y_{\dot{v}}, Z_{\dot{w}}$ coefficients respectively.

The obtained forces diagram in x,y,z directions are shown in following figures:

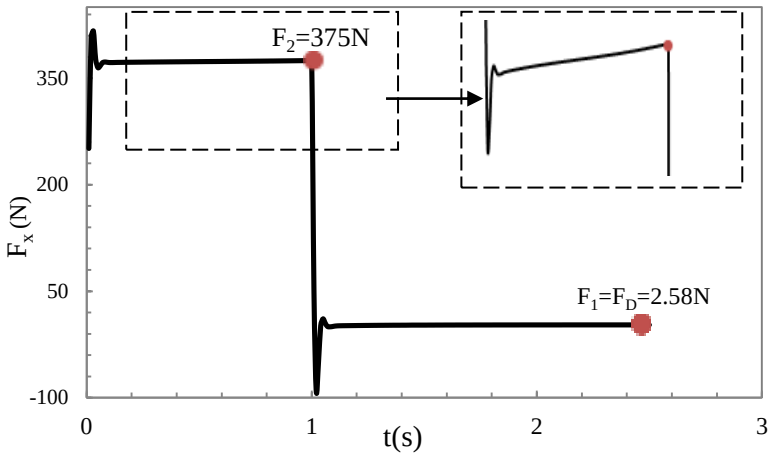

Figure 5: Acted force in the surge motion of the Suboff

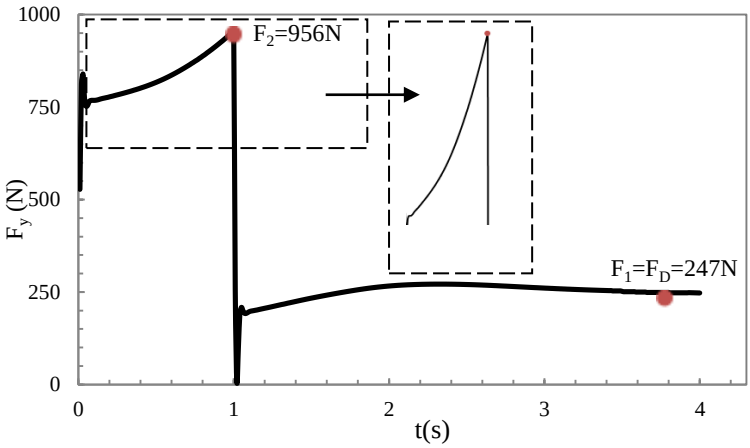

Figure 6: Acted force in the sway motion of the Suboff

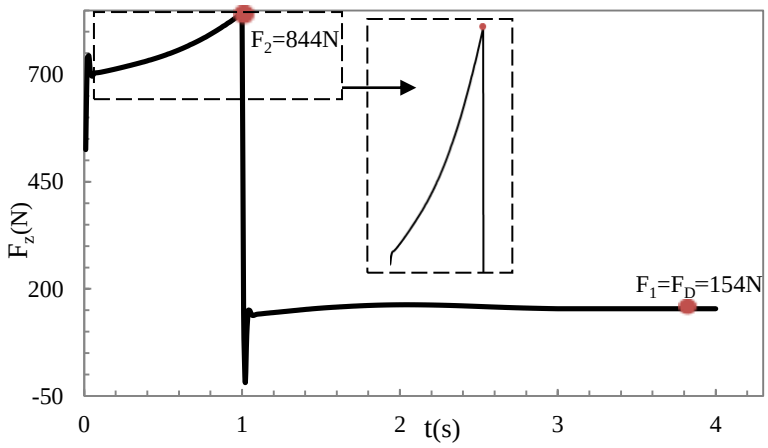

Figure 7: Acted force in the heave motion of the Suboff

A cubic fluid domain is established according to the real scale of submarine, and consists of:
-Surge motion: one model length at up-stream, four model lengths at downstream and outer domain's walls is located at the eight-model diameter away from the submarine.
-Sway and heave motions: three model diameters at up-stream, fifteen model diameters at downstream and outer domain walls are located at the twice model length.
After the initial unstable region in the accelerated motion, the forces are linearly increased, but the scale of the curves prevents to see this increment easily. Note that, the oscillations in the surge force are smoother because of the streamlined shape of submarine in longitudinal direction.

Analytical calculations
As it explained, the area moment of inertia is used to obtain two diameters of the hull and appendages. The hull has port-starboard symmetry about x-z plane, and top-bottom symmetry about x-y plane; therefore, the hull should be replaced by a prolate ellipsoid of revolution ($b=c<a$). Two diameters of ellipsoid are determined by calculating the area moments of segment shown in the figure 8.

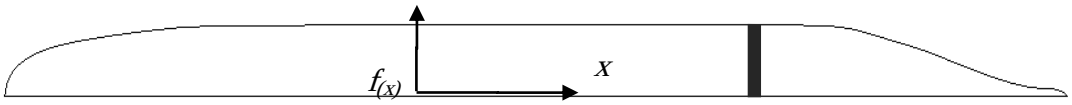

Figure 8: sheer profile of the hull and differensial vertical strip

If the local height of the hull is approximated by a 4th degree polynomial

$$f_{(x)} = -0.0156x^4 + 0.0113x^3 + 0.0208x^2 - 0.0273x + 0.2525 \tag{12}$$

Using a diffrensial vertical strip with the height $f_{(x)}$ and width dx, the area moments of inertia at the area center of the hull are expressed as:

$$\int \frac{1}{3} f_{(x)}^3 dx = 0.5 I_{x(ellipse)} = \frac{\pi}{8} ab^3$$
$$\int x^2 f_{(x)} dx = 0.5 I_{y(ellipse)} = \frac{\pi}{8} a^3 b \tag{13}$$

There are two equations in two unknowns; therefore, a,b can be calculated and consequently $c=b$. Similar procedure is implemented for the appendages. Because of the rectangular shape of the sail, the dimensions of the replacement ellipse

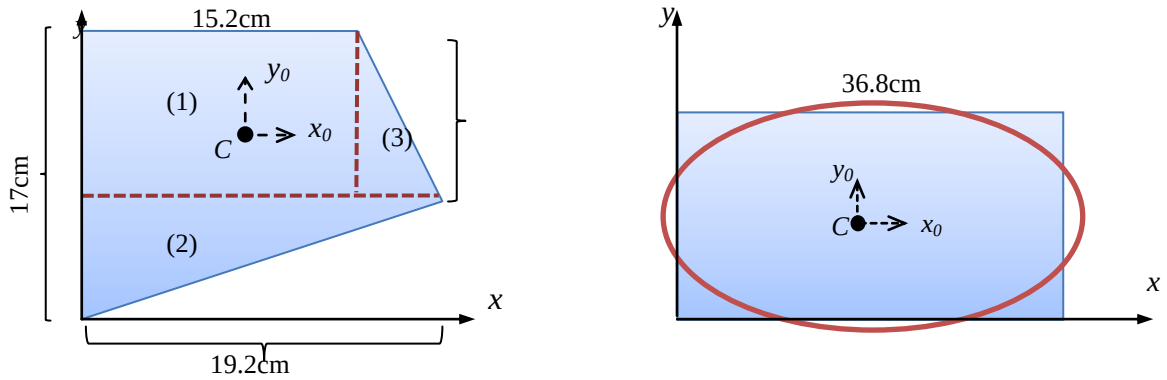

Figure 9: Drawing of the control surface and sail

are simply calculated by equaling the area moments of inertia for both geometries.
However, when an area is composed of many parts, it is convenient to tabulate the results for each part. Here, the control surface area is composed of the rectangle (1) and the triangles (2) and (3). The area moments of inertia about the centroidal axes with origin at *C*=(8.03,9.14) are calculated as follow:

Table 5: mathematical properties of the control surface

Part	A (cm^2)	d_x (cm)	d_y (cm)	Ad_x^2	Ad_y^2	$\bar{I}_x$ (cm^4)	$\bar{I}_y$ (cm^4)
(1)	155.04	0.43	2.76	28.66	1181.03	1344.2	2985
(2)	65.28	1.63	4.6	173.44	1381.32	167.7	1336.9
(3)	20.4	8.5	1.06	1473.9	22.92	117.9	18.1
∑				1676	2585.27	1629.8	4340

d is the distance from centroidal axis of each part to the axis about which the moment of inertia of the entire section is to be computed. Thus, the area moments of inertia for the control surface about centroidal x_0- and y_0-axes become

$$I_{x_0} = \sum \bar{I}_x + \sum Ad_x^2$$
$$I_{y_0} = \sum \bar{I}_y + \sum Ad_y^2 \qquad (14)$$

Now, the calculated area moment of inertia similarly should be equivalent to its replacement ellipse. Note that, maximum thickness is the third diameter for the sail and control surfaces. The obtained diameters are specified in table6.

Table 6: Dimension of replaced ellipsoids for various components of submarine

	hull	sail	rudder	stern
a (*cm*)	218	21	10.6	10.6
b (*cm*)	27	6.7	3	7.3
c (*cm*)	27	11.7	7.3	3

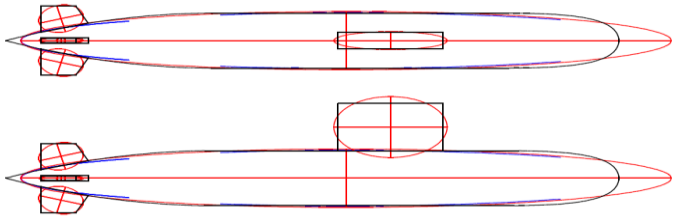

Figure 10: Replacement of submarine with a series of ellipsoids

Results and discussions

In the table7, the computed added mass coefficients by numerical simulation and analytical approach are compared with DTRC experimental reports [9] and published PMM results [12]. The added mass coefficients become dimensionless by dividing to $\frac{1}{2}\rho l^3$.

Table 7: Comparison of the linear added mass coefficients

	Present numerical work	Present analytical work	Exp reports	PMM result
$X'_{\dot{u}}$	0.6×10^{-3}	0.4×10^{-3}	-	-
$Y'_{\dot{v}}$	0.017	0.014	0.016	0.019
$Z'_{\dot{w}}$	0.016	0.0135	0.014	0.018

According to the table7, the results of present numerical method are close to the experimental and PMM results; nevertheless, the time of computations is less due to simplicity of simulations. Numerical representing of sinusoidal motions complicates the PMM simulations, and subsequently increases the time of calculations.

Conclusions

In this paper, using the unsteady RANS simulation, the linear added mass coefficients for a submarine were calculated numerically in axial and lateral directions. In order to verify the method, its results were compared with the expected results for a sphere. The numerical results agreed well with the available experimental results of the submarine. However, this method was simple and low-cost in comparison to the PMM simulation for calculating the corresponding coefficients. In addition, an analytical approach was used to determine the diagonal added mass coefficients of mentioned submarine. It was demonstrated that the moments of inertia was a good criterion for choosing the best dimensions of the replacement ellipsoids. Note that, both methods are exclusively applied in calculating the coefficients in deep water.

List of Symbols

C_P	pressure coefficient
f	body force
i,j	displacement directions index
u_i'	fluctuating velocity

Greek symbols

ρ	Density

Reference

[1] Doug Perrault, Neil Bose, SiuO'Young, Christopher D. Williams, " *Sensitivity of AUV added mass coefficients to variations in hull and control plane geometry* ", Ocean Engineering, Volume 30, Issue 5, Pages 645-671, April 2003.

[2] Zhiliang Lin, Shijun Liao, "*Calculation of added mass coefficients of 3D complicated underwater bodies by FMBEM* ", Commun Nonlinear Sci Numer Simulat, Volume 16, Pages 187-194.

[3] D,Watt "*Estimates for the added mass of a multi component deeply submerged vehicle* " Technical Report, national defence, canada 1988.

[4] He Zhang, Yu-ru Xu and Hao-peng Cai, "*Using CFD Software to Calculate Hydrodynamic Coefficients*", J. Marine. Sci. Appl. (2010).

[5] Phillips, A.B., Furlong, M. and Turnock, S.R. "*Virtual planar motion mechanism tests of the autonomous underwater vehicle autosub*". In, STG-Conference/Lectureday "CFD in Ship Design", Hamburg, Germany, Sep 2007.

[6] Zhao Jinxin, Su Yumin, Ju Lei, Cao Jian, "*Hydrodynamic Performance Calculation and Motion Simulation of an AUV with Appendages*", International Conference on Electronic & Mechanical Engineering and Information Technology 2011.

[7] A. C. Hochbaum, "*Virtual PMM Tests for Manoeuvring Prediction* " presented at the 26th Symposium on Naval Hydrodynamics, Rome, Italy, 2006.

[8] Seong-Keon Lee, Tae-Hwan Joung," *Evaluation of the added mass for a spheroid-type unmanned underwater vehicle by vertical planar motion mechanism test* ", Inter J Nav Archit Oc Engng (2011).

[9] Roddy. R. F. "*Investigation of the stability AMD control characteristic of several configuration of the darppa suboff model*". Ship Hydromechanics Department Report 1990.

[10] A.C. Fernandesa, F.P.S. Mineirob," *Assessment of hydrodynamic properties of bodies with complex shapes*", Applied Ocean Research 29 (2007).

[11] Alexandr L.Korotkin." *Added Mass of Ship Structures*" Krylov Shipbuilding Research Institute, Russia, 2007.

[12] Pan Yu-cun, "*Numerical prediction of submarine hydrodynamic coefficient using CFD simulation*", Department of Naval Architecture, Naval University of Engineering, China, journal of hydrodynamic, Page 840-847, September 2012.